Surface-Roughness Evolution During the Cementation of Silver Ions on Solid Copper in Aqueous Sulfuric Acid Solution

by **Grzegorz D. Sulka*** and **Marian Jaskuła**

Department of Physical Chemistry, Faculty of Chemistry, Jagiellonian University, Ingardena 3, PL-30-060 Krakow
(phone: +48-12-663-2266; fax: +48-12-634-0515; e-mail: sulka@chemia.uj.edu.pl)

The evolution of the surface roughness during cementation of Ag^+ conducted either in O_2-free or O_2-saturated aqueous $H_2SO_4/CuSO_4$ was investigated at two different initial concentrations of Ag^+. The kinetics data of the process determined previously in the rotating cylinder were linked directly with scanning-electron-microscope (SEM) images and surface-height-distribution diagrams calculated for various cementation times. It was found that, at the beginning of the process, the surface roughness decreases due to formation of a flat Ag layer on the top of the surface, independent of the presence or absence of O_2 in the system. With increasing reaction time, an increase in the surface roughness was observed. The rate enhancement of the process is mainly responsible for the increase of the surface roughness in the O_2-saturated solutions, especially at the higher initial Ag^+ concentration (100 mg/dm^3). The rate enhancement observed at a latter stage of the process, connected with the increase of the effective surface area of the cathodic sites, was separated from the rate enhancement induced by the competitive chemical process occurring in O_2-free solution. The difference in the mechanisms of the processes conducted under aerobic and anaerobic conditions was reflected in the surface-heigth distributions calculated from the SEM images.

Introduction. – Cementation is an electrochemical process in which a more-electropositive metal ion present in solution is reduced by an electronegative solid metal. Due to the simplicity of the reaction conditions in various industrial processes and due to its low-energy consumption, cementation is commonly used for recovery of valuable [1–5] and precious metals [6–11] from the leach liquors and wastewaters. Cementation processes are often employed for purification of electrolytes used for electrodeposition of high-purity metals [12–14] as well as for removal of toxic metal species and soluble heavy-metal ions presented in aqueous solutions [15–18]. The overall reaction for silver (Ag) cementation on copper (Cu) is expressed by the following equation:

$$2\,Ag^+ + Cu^0 \rightarrow 2\,Ag^0 + Cu^{2+} \quad (1)$$

This is a heterogeneous redox reaction involving reduction of Ag^+ at cathodic sites on the Cu surface, and dissolution of Cu at anodic sites on the same metallic surface. It is generally accepted that this type of cementation follows first-order kinetics, and is limited by the diffusion of Ag^+ to the Cu surface at the initial stage of the process. However, the structure and morphology of the reaction product formed during the initial stage have a significant influence on the kinetics of the process in the latter stage, either enhancing the rate in some cases [19–28] or passivating the surface in others

[19][26][29]. In nitrate, sulfate, or perchlorate solutions, rate enhancement was observed, but a passivating effect of the Ag deposit was observed in cyanide or chloride solutions. The enhanced cementation rate results usually from the enhancing effect of the growing deposit by increasing the effective surface area [20–26], thus increasing the roughness of the deposit and the rate of the mass transfer [19][23][26–28]. The decrease of the overall reaction rate is attributed to the blocking effect of the growing Ag cement [19], lower diffusion rate of Ag complexes [26], and a chemical, competitive process [19][26].

It is worth considering that the starting surface area of the metallic Cu can be easily modified and significantly enlarged by a relatively high concentration of Ag^+, as commonly used in cementation. In the latter case, especially when the reacting surface area is small, a separation and determination of the rate-enhancing factor seems to be impossible.

The cementation of Ag^+ on Cu has been studied before in neat H_2SO_4 solution [30][31]. Also, the influence of the concentration of Cu^{2+} and of O_2 in the system on the kinetics of cementation was discussed. The kinetics and mechanism of Ag cementation on Cu in 0.5M H_2SO_4 solution containing 0.5M $CuSO_4$ were reported in previous papers [32][33]. To avoid the unwanted effect of high Ag^+ concentrations and small surface areas, the study was performed in a solution containing either 20 or 100 mg/dm^3 of Ag^+ in a rotating cylinder system with a relatively large surface area. It was found that the cementation reaction at the initial stage of the process follows first-order kinetics. At a latter stage, the kinetics and mechanism strongly depends on the presence of O_2 in the system. Under anaerobic conditions, a competitive reaction between Ag^+ and Cu^+, enhancing the kinetics of the process, can occur in bulk solution. Therefore, the initial Ag^+ concentration influences the morphology of the Ag deposit. On the contrary, the presence of O_2 does not affect significantly the morphology of cemented Ag.

In the present study, we have developed a new approach for studying the surface-roughness evolution during the cementation process. The observed results are linked with the mechanism of the process.

Experimental. – Reagent-grade chemicals and four times dist. H_2O were used to prepare all solns. Cementation experiments were carried out in a rotating-cylinder system described previously [32]. The rotating cylinder provides similar turbulent mass-transport conditions even if the roughness of the deposit increases significantly. The working surface area of the rotating cylinder was 27.50 cm^2. Before each run, the rotating steel cylinder was immersed in HNO_3/H_2O 1:1 (*v*/*v*), rinsed with H_2O, and degreased in MeOH. Then, it was covered electrolytically with a fresh, 24-μm thick layer of Cu. The deposition of Cu was carried out at const. current density (36.4 mA/cm^2) for 30 min at 20° in an electrolyte containing 0.5M H_2SO_4 and 0.5M $CuSO_4$. To obtain a smooth and flat initial reaction surface, the deposited Cu layer was electropolished in H_3PO_4/H_2O 3:1 at const. current density (72.7 mA/cm^2) for 40 s at 20°, and then chemically polished in 0.5M H_2SO_4 soln. After polishing, the cylinder was rinsed, dried, and used for cementation. All pre-treatment procedures have been described in detail in [32][33].

Cementation was investigated in an electrolyte made of 0.5M H_2SO_4 and 0.5M $CuSO_4$ at 25°. The soln. was stirred at a controlled speed of 500 r.p.m. The initial concentration of Ag^+ in soln. was either 20 or 100 mg/dm^3, and was determined before the experiment by atomic-absorption spectroscopy (AAS). The volume of the electrolyte in the cell was 0.2 dm^3. Before each run, the electrolyte in the cell was purged by bubbling with high-purity Ar or O_2 gas for 20 min. The O_2-free or O_2-sat. atmosphere was maintained over the soln. throughout the whole process by continuously passing Ar or O_2.

The duration of the experiments was adjusted depending on the initial Ag^+ concentration. At 20 mg/dm^3 Ag^+, samples were analyzed after 7, 14, 21, 30, 40, 50 and 60 min. When the initial Ag^+ concentration was 100 mg/dm^3, the experiment was terminated after 5, 10, 15, 20, 30, 45, and 60 min. After each run, the Cu layer with cemented Ag was rinsed carefully, dried, cut, and separated from the cylinder. Samples of the Cu sheet with cemented Ag were then dissolved in hot HNO_3/H_2O 1:1, and analyzed for Ag content by AAS. For each cementation test, the surface of two samples of the Cu sheet with cemented Ag was inspected with a *Phillips XL-30* scanning electron microscope (SEM). SEM Images were analyzed with the scanning-probe image processor WSxM 3.0 Beta [34].

Results and Discussion. – The surface-roughness evolution during Ag^+ cementation on Cu was investigated under O_2-free (anaerobic) and O_2-saturated (aerobic) conditions at either 20 or 100 mg/dm^3 Ag^+. In *Fig. 1*, the SEM top-view images of the Cu surface with cemented Ag resulting from 20 mg/dm^3 Ag^+ under O_2-free conditions is shown, together with the corresponding surface-height-distribution diagrams taken at various time intervals. The analyzed surface area of the samples was *ca.* 500 μm^2. To better understand the evolution of the surface roughness with cementation time, a semi-quantitative analysis of the surface–height distribution was performed. The peak width at half peak height, $W_{1/2}$, was measured for all histograms (*Fig. 1*).

At the beginning of the cementation process, some parts of the Cu surface are covered with metallic Ag, but some parts still remain uncovered. The parts of the surface with deposited Ag behave as cathodic sites, where the deposition of the noble metal occurs. The uncovered Cu surface plays the role of the anodic site, where dissolution of Cu takes place. The dark spots in the SEM image taken after 7 min (*Fig. 1*, *a*) represent anodic sites and/or relatively deep cavities on the surface. These spots are distributed rather uniformly over the surface area. The distribution histogram of the surface height calculated from this non-homogeneous surface shows a relatively wide peak ($W_{1/2}=0.208$), with a wide range of surface heights existing on the top of the analyzed surface. Especially, a negative-height region in the diagram (dark spots in the SEM image) varies significantly. After 21 min of cementation (*Fig. 1*, *b*), the surface is fully covered with Ag, and the anodic sites are fully developed and spread over the surface as a net of cracks. It was previously found that anodic sites develop their working surface area in the Cu material just under the deposited Ag, with formation of cavities under the surface [33]. After 21 min, the Ag crystals found on the surface are tiny, covering the surface uniformly and compactly. As a result, the surface-height analysis of the SEM image shows a narrow and intense peak (*Fig 1*, *b*; $W_{1/2}=0.168$).

The surface roughness changes once again after 40 min (*Fig. 1*, *c*). As expected, the cemented Ag now forms a thicker, less-uniform layer on the top of Cu, and, consequently, a broader peak appears in the surface-height-distribution diagram ($W_{1/2}=0.243$). Further extension of the process duration to 60 min does not change significantly the roughness of the Ag deposit (*Fig. 1*, *d*). The half-width of the peak ($W_{1/2}=0.230$) is comparable with that obtained after 40 min. This can be attributed to the percentage of cemented Ag on Cu (relative to the initial Ag content determined by AAS) remaining almost constant after 30 min under anaerobic conditions at 20 mg/dm^3 Ag^+. In the distribution diagram of the surface heights presented in *Fig. 1*, *d*, some surface heights, especially in the positive range of the diagram, create an additional subdiagram. This can be attributed to a rather incidental regularity of the change

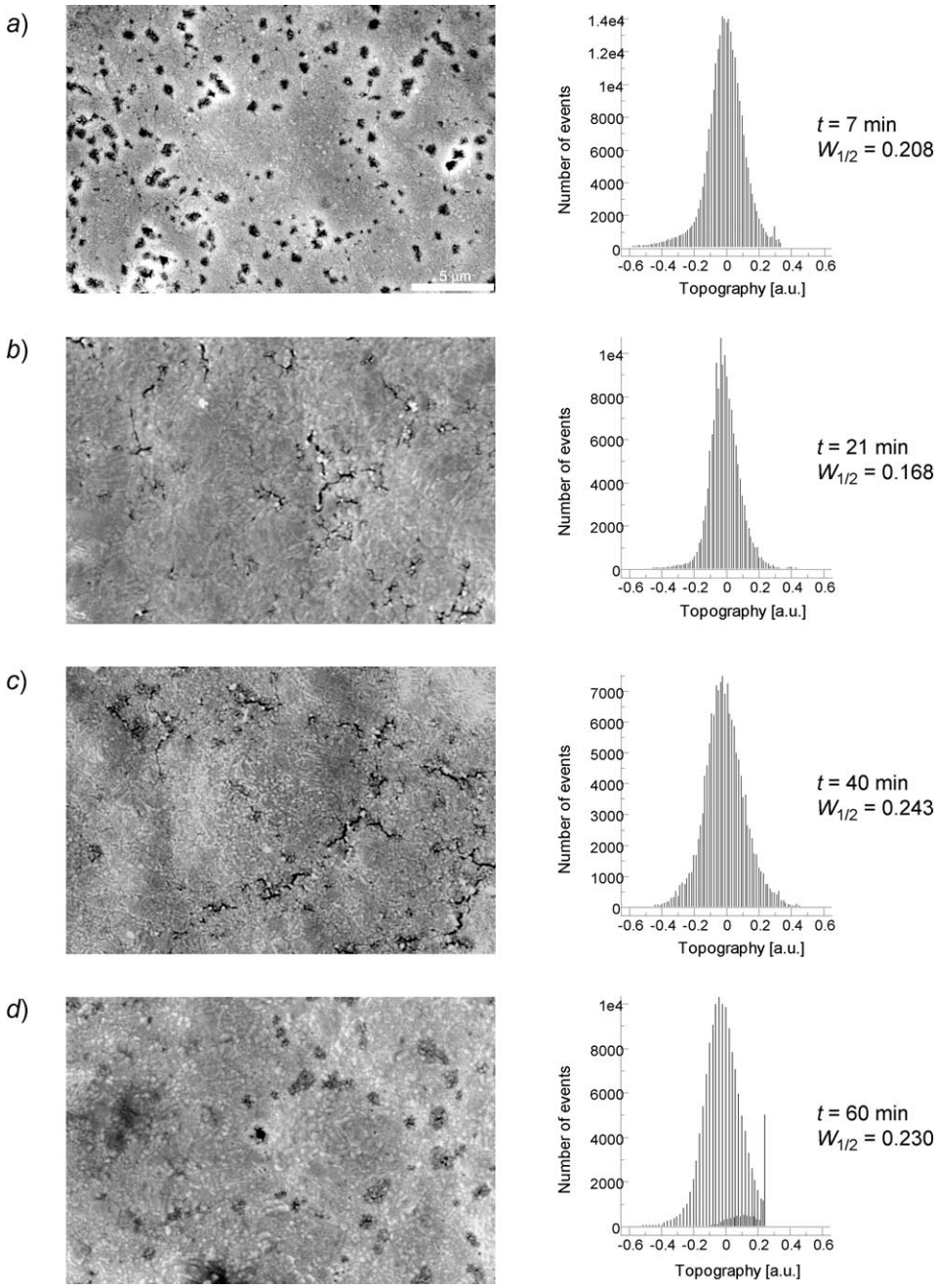

Fig. 1. *SEM Top-view images and surface-height-distribution diagrams for Ag cementation in an O_2-free solution.* $[Ag^+]_0 = 20$ mg/dm^3, electrolyte: 0.5M H_2SO_4/0.5M $CuSO_4$, $T = 25°$; process time: 7 min (*a*), 21 min (*b*), 40 min (*c*), 60 min (*d*).

in Ag grain size. As will be seen later, the surface-roughness evolution with cementation time is closely connected with the mechanism of this process.

In *Fig. 2*, the SEM top-view images of the Cu surface with Ag deposit formed under *aerobic* conditions at 20 mg/dm^3 Ag^+ ion are shown. In the presence of O_2, besides the cementation reaction occurring on the Cu surface, corrosion of Cu takes place. Comparison of the corresponding SEM images presented in *Figs. 1* and *2* for the same time intervals shows that the presence of O_2 does not modify significantly the morphology of Ag cement formed on the top of the surface. The only difference is the degree of corrosion of Cu and the formation of anodic sites seen as a dense net of cracks (*Fig. 2*,*d*). Anodic sites are also clearly visible on the top of the sample obtained after 7 min, when carried out in O_2-saturated solution (*Fig. 2*,*a*). Due to the enhanced Cu corrosion, the surface-height distribution calculated from the SEM image shown in *Fig. 2*,*a* shows a broader peak compared to that presented in *Fig. 1*,*a*.

After 21 min of cementation, a flattening effect of the Ag deposit appears (*Fig. 2*,*b*), and the value of $W_{1/2}$ decreases. Now, the Ag deposit covers granular Cu crystals with a uniform layer. As a result, a narrow and intense peak in the surface-height-distribution diagram appears. Anodic sites, visible as cracks on the surface, are already fully developed. Further cementation of Ag on the Cu surface leads to an increase in the thickness of the Ag deposit and its roughness. Larger Ag crystals on the surface appear, and the peak in the distribution diagram broadens a little (*Fig. 2*,*c*). Finally, after 60 min, the narrow peak in the surface-height-distribution diagram (*Fig. 2*,*d*) indicates, in a qualitative fashion, another flattening effect of the Ag deposit.

To better understand the surface-roughness evolution during Ag^+ cementation on Cu (*Figs. 1* and *2*), deeper insight into the kinetics data and mechanism of the process is necessary. The *Table* below shows the average percentage of cemented Ag as a function of cementation time for both O_2-free and O_2-saturated conditions, and for initial Ag^+ concentrations of 20 or 100 mg/dm^3. As can be seen, at 20 mg/dm^3 initial Ag^+, the difference in cemented Ag gets more pronounced after 21 min of process duration for the aerobic *vs.* anaerobic systems. This is in agreement with the observation that, after 21 min, there are smooth Ag deposits on the Cu surface, with a narrow peak in the surface-height-distribution diagram, in both cases (*Figs. 1*,*b* and *2*,*b*). This can be attributed to the Cu surface being covered with tiny, uniform Ag crystals and a somewhat flattened surface roughness. This result is consistent with kinetics data obtained previously [32]. There, we had reported that the presence or absence of O_2 does not modify the kinetics of the process at the *initial* stage of cementation, *i.e.*, during the first 10–12 min. At a latter stage, a rate enhancement had been observed, mainly for cementation conducted in O_2-free solution. For the later stage, the enhancement factor, defined as the ratio of actual to initial reaction rate, was estimated at *ca.* 1.08 and 1.02 for the O_2-free and O_2-saturated solutions, respectively [32].

During cementation, the surface roughness increases due to the observed slight rate enhancement, which induces an increase in the size of the Ag crystals, as well as due to the increasing depth of the anodic sites. The increase in surface roughness is indicated by peak broadening in the distribution diagrams (*Figs. 1*,*c* and *2*,*c*).

Two questions arise after examination of the *Table*. Why does the smaller rate observed under aerobic conditions at 20 mg/dm^3 Ag^+ lead to a higher percentage of cemented Ag after 40 min? And, *vice versa*, why is there a lower percentage of

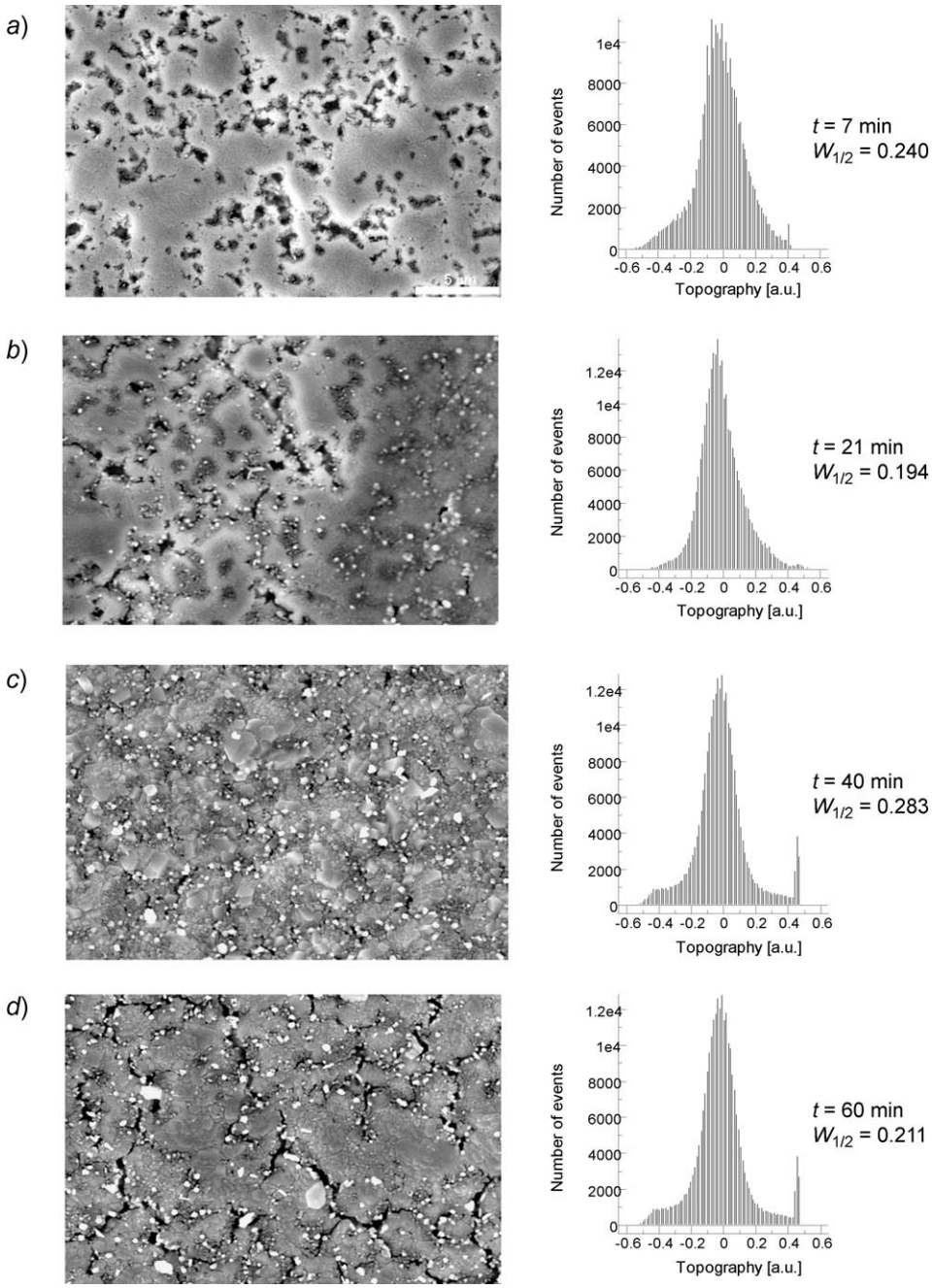

Fig. 2. *SEM Top-view images and surface-height-distribution diagrams for Ag cementation in an O_2-saturated solution.* $[Ag^+]_0 = 20$ mg/dm^3, electrolyte: 0.5M H_2SO_4/0.5M $CuSO_4$, $T = 25°$; process time: 7 min (*a*), 21 min (*b*), 40 min (*c*), 60 min (*d*).

Table. *Percentage of Cemented Silver on Copper Determined by AAS under Oxygen-Free and Oxygen-Saturated Conditions as a Function of Process Time.* $T = 25°$, $f = 500\ min^{-1}$. For details, see *Experimental*.

t [min]	$[Ag]_0 = 20$ mg/dm^3 [a])		t [min]	$[Ag]_0 = 100$ mg/dm^3 [a])	
	O_2-free	O_2-sat.		O_2-free	O_2-sat.
7	17.0 ± 1.0	15.2 ± 0.4	5	12.6 ± 0.6	13.7 ± 0.2
14	28.8 ± 0.6	28.5 ± 0.3	10	33.6 ± 0.2	31.9 ± 1.9
21	40.1 ± 0.8	39.3 ± 0.9	15	55.8 ± 0.3	54.3 ± 0.4
30	46.5 ± 1.9	53.0 ± 0.8	20	64.9 ± 0.6	66.8 ± 1.7
40	45.2 ± 4.4	61.3 ± 1.6	30	73.5 ± 2.9	91.4 ± 0.4
50	40.9 ± 2.8	66.4 ± 2.7	45	72.1 ± 0.9	92.2 ± 0.1
60	48.2 ± 5.0	72.9 ± 0.8	60	77.8 ± 0.4	93.7 ± 1.1

[a]) Initial Ag^+ solution concentration.

cemented Ag after the same period of time for the higher-rate enhancement found under anaerobic conditions? As can be seen from the *Table*, the percentage of cemented Ag, calculated for the O_2-saturated solutions, gradually increases with cementation time, but quickly reaches a plateau for the O_2-free solutions (41–48% after 30 to 60 min). These results are in very good agreement with a mechanism we had proposed previously [33]. The mechanism of Ag^+ cementation on Cu in aqueous H_2SO_4 solution depends on the presence of O_2, and consists of two reaction stages. In the first step, and independent of the presence of O_2, adsorbed Cu^+ (Cu^+_{ad}) is generated directly on the Cu surface according to the following reaction:

$$Ag^+ + Cu^0 \rightarrow Ag^0 + Cu^+_{ad} \tag{2}$$

The second step of the cementation reaction, however, strongly depends on the presence or absence of O_2. In an O_2-saturated solution, the adsorbed Cu^+ species either react with Ag^+ (*Eqn. 3*) or are immediately oxidized by O_2 (*Eqn. 4*).

$$Cu^+_{ad} + Ag^+ \rightarrow Cu^{2+} + Ag^0 \tag{3}$$

$$4\ Cu^+_{ad} + 4\ H^+ + O_2 \rightarrow 4\ Cu^{2+} + 2\ H_2O \tag{4}$$

The front of the reaction is strictly located at the reaction surface. For the O_2-free solution, the generated Cu^+_{ad} ions can react immediately with Ag^+ (*Eqn. 3*) or diffuse into the bulk solution to react as dissolved (soluble) Cu^+_{sol} ions with Ag^+. The latter process is represented by the following equations:

$$Cu^+_{ad} \rightarrow Cu^+_{sol}\ (\textit{via}\ \text{diffusion}) \tag{5}$$

$$Cu^+_{sol} + Ag^+ \rightarrow Cu^{2+} + Ag^0_{colloid} \tag{6}$$

The front of the above reaction can move from the surface towards the bulk of the solution. The progress of the competitive reaction (*Eqn. 6*) consuming additional Ag^+ is

the main reason why the percentage of cemented Ag remains low and almost constant between 30 and 60 min (*Table*). These results are confirmed by the broad peak in the surface-height-distribution diagram observed after 60 min (*Fig. 1*, *d*). The roughness of the deposit does not change significantly between 40 and 60 min under O_2-free conditions. On the contrary, the narrow peak in the diagram (*Fig. 2*, *d*) is obtained after 60 min of cementation in O_2-saturated solution. This suggests a development of a denser, more-packed Ag deposit on Cu in the cementation process conducted in O_2-saturated solution. And it is consistent with the kinetics data showing that there is a slight decrease of the enhancement factor after 30 min of reaction [32]. Taking into account that the front of the cementation reaction cannot move from the surface towards the bulk of the solution, the formation of a compact Ag deposit can be expected in the presence of O_2.

In *Fig. 3*, higher-magnification SEM top-view images of the surface with Ag deposit are shown for 60 min of cementation for the O_2-free (*a*) and O_2-saturated (*b*) solutions. The initial Ag^+ concentration in solution was 20 mg/dm^3. Additionally, a SEM line-scan analysis of the anodic sites was performed, and the intensity profile along the direction indicated in the SEM images are presented. Profile analysis shows that there is no significant difference in the breadth of cracks on the surface. The average breadth of the cracks is 0.33 and 0.58 μm for the O_2-free and O_2-saturated solutions, respectively. This suggests that the anodic sites develop their surface area under the surface towards the basic Cu material, as observed in a previous study [33]. Further, it can be seen from *Fig. 3* that the Ag cement exhibits a granular structure with small- and medium-sized crystals on the surface, independent of the presence or absence of O_2. However, the profile analysis performed from the SEM images exhibits an interesting, but small difference in the deposit morphology. Under aerobic conditions, more peaks are recorded in the profile than for the anaerobic system. This can be rationalized in terms of a slightly different rate enhancement of the process, and by deposition of finer Ag crystals on the surface during the cementation conducted in the presence of O_2.

In *Figs. 4* and *5*, the SEM images of the sample surface and their surface-height distributions are shown for an initial Ag^+ concentration of 100 mg/dm^3 at various reaction times for O_2-free and O_2-saturated solutions, respectively. The measured peak half-width is also shown. The surface area used for the surface-height analysis was *ca.* 0.7 mm^2. A general examination of the SEM images shown in *Figs. 4* and *5* leads to the conclusion that the presence of O_2 does not influence the morphology of the Ag deposit. At this particular magnification, the dendrites look similar under both aerobic and anaerobic conditions. The rate enhancement of the process can be expected to be significant only in the latter stage of the process, based on the increasing surface area of cathodic sites. Indeed, the enhancement factor for the latter-stage process was estimated at *ca.* 2.2 and 3.6 for O_2-free and O_2-saturated solutions, respectively [32]. The increasing surface roughness with cementation time is clearly visible from the SEM images.

As can be seen from *Figs.* 4, *a* and *5*, *a*, both taken after 10 min, relatively huge dendrites appear on the surface. At this stage, the Cu surface is completely covered with a Ag layer, and cathodic sites start their growth from the surface protrusions developing significantly their surface area. The surface is highly heterogeneous, and the calculated distribution histogram of the surface height shows peaks with a significant contribution of various dendrite heights in the range of positive values (*Figs. 4*, *a* or *5*, *a*). The surface

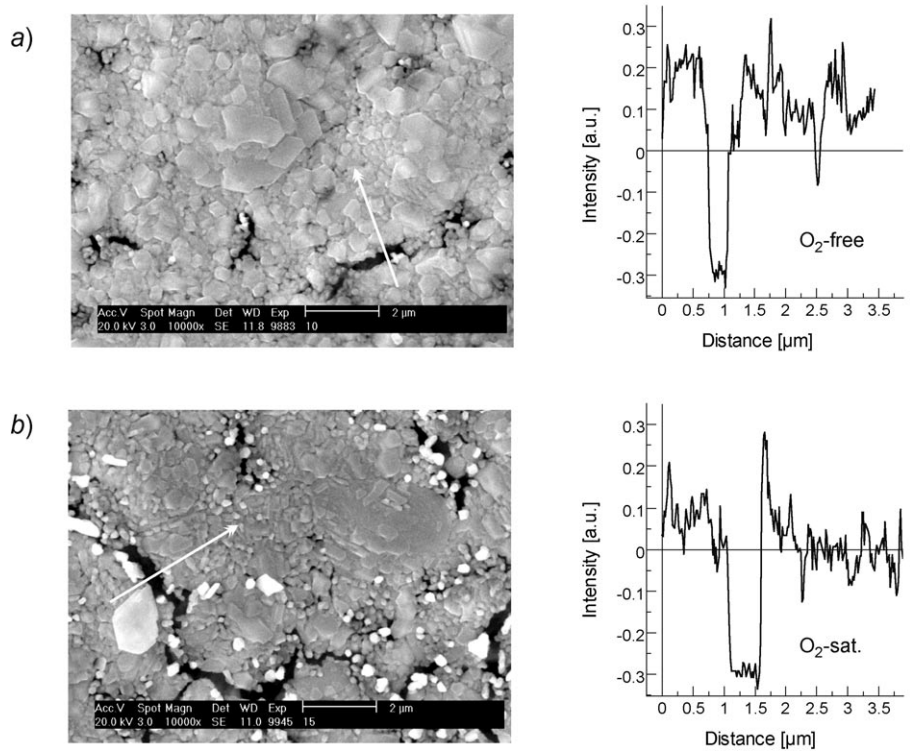

Fig. 3. *SEM Top-view images with anodic sites and line-scan analysis along the marked direction for Ag cementation after 60 min in* a) *O_2-free and* b) *O_2-saturated solution.* $[Ag^+]_0 = 20$ mg/dm^3, electrolyte: 0.5M H_2SO_4/0.5M $CuSO_4$, $T = 25°$.

area occupied by dendrites and, consequently, the area of cathodic sites, increase with increasing reaction time under both O_2-free and O_2-saturated conditions. The increasing number of dendrites formed on the reaction surface and their size and height evolutions result in a peak broadening in the surface-height-distribution diagram with increasing cementation time (*cf.* $W_{1/2}$ in *Figs. 4,a–4,c* or *5,a–5,c*).

From SEM images taken at identical reaction times, *e.g.*, after 10 or 20 min (*Figs. 4,a* and *5,a*, or *Figs. 4,b* and *5,b*), it can be seen that the number of dendrites on the surface is similar, independent of the presence or absence of O_2. These results are consistent with the percentage of cemented Ag found on the reaction surface for an initial Ag^+ concentration of 100 mg/dm^3 (*Table*). There is no observable difference in the percentage of Ag on the reaction surface found after the cementation test conducted in the presence or absence of O_2 for reaction times not exceeding 30 min. The difference in the percentage of cemented Ag calculated for the aerobic and anaerobic processes is clearly visible for the range of cementation time between 30 and 60 min. In all of these experiments, the percentage of cemented Ag does not exceed 78% and 94%, respectively, for the anaerobic and aerobic solutions. The lower value (78%) is closely related to the mechanism of the process, and especially to the competitive reaction pre-

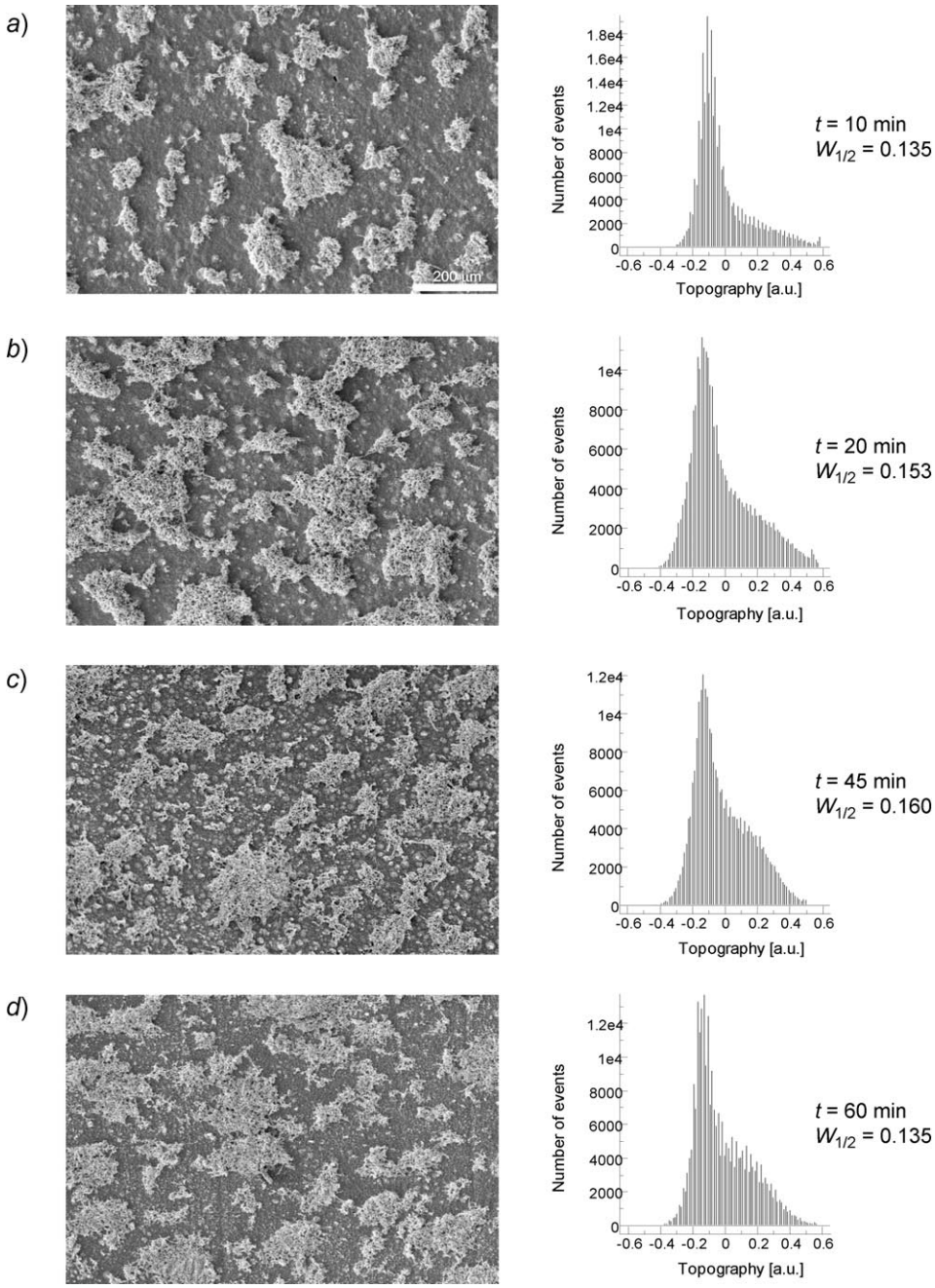

Fig. 4. *SEM Top-view images and surface-height-distribution diagrams for cementation at high Ag^+ concentration in an O_2-free solution.* $[Ag^+]_0 = 100$ mg/dm^3, electrolyte: 0.5M H_2SO_4/0.5M $CuSO_4$, $T = 25°$; process time: 10 min (*a*), 20 min (*b*), 45 min (*c*), 60 min (*d*).

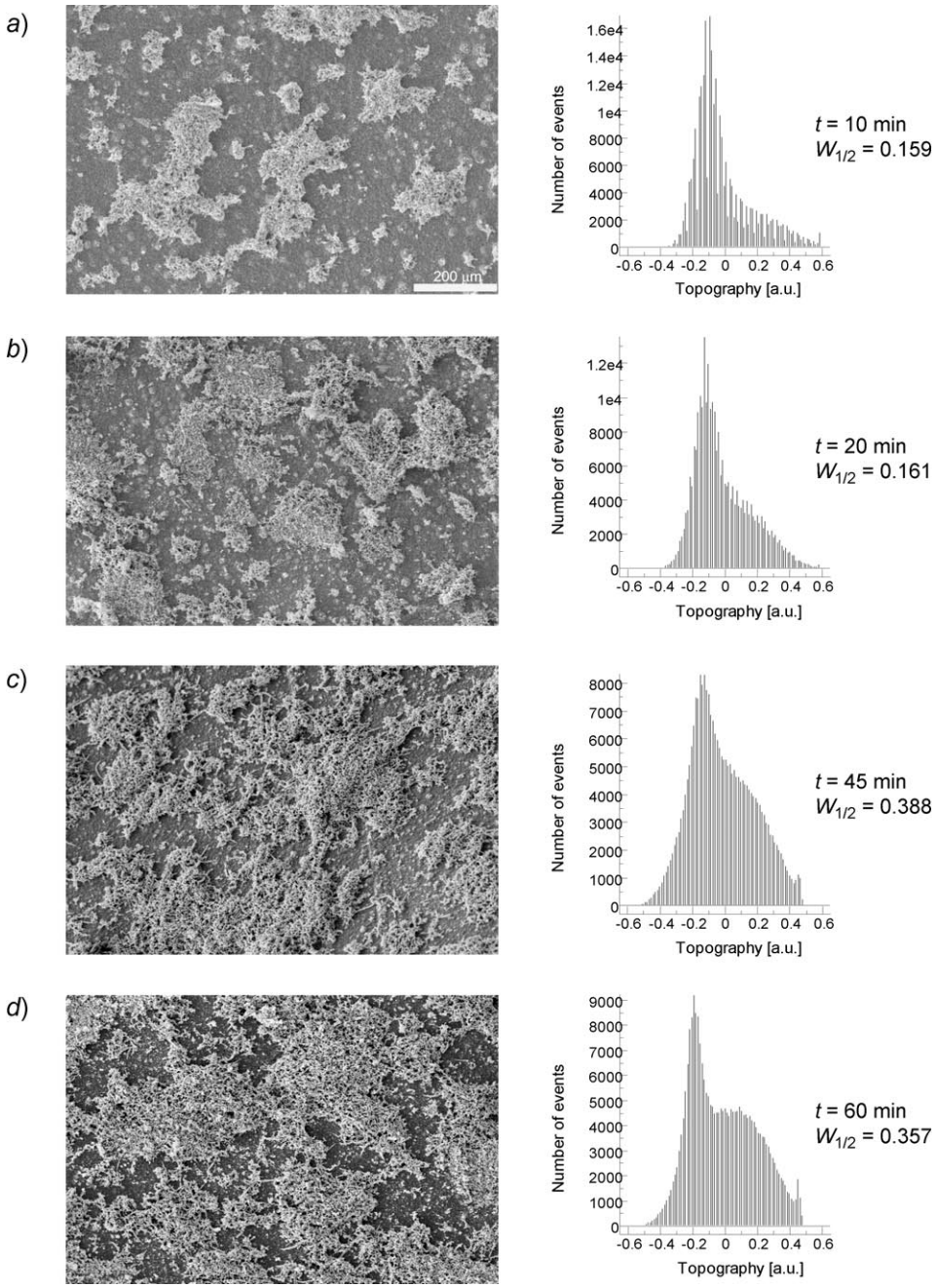

Fig. 5. *SEM Top-view images and surface-height-distribution diagrams for cementation at high Ag^+ concentration in an O_2-saturated solution.* $[Ag^+]_0 = 100$ mg/dm^3, electrolyte: 0.5M H_2SO_4/0.5M $CuSO_4$, $T = 25°$; process time: 10 min (*a*), 20 min (*b*), 45 min (*c*), 60 min (*d*).

sented in *Eqn. 6* occurring in bulk solution. The contribution of this reaction to the overall kinetics of the process was estimated at *ca*. 40% [32]. This difference in the percentage of cemented Ag is indicated also in the distribution diagrams of the surface height. For O_2-free conditions, a narrower peak is observed ($W_{1/2}$ in *Figs. 4,c* or *4,d*) in comparison to the one obtained for the same time period it the presence of O_2 (*Figs. 5,c* or *5,d*).

Conclusions. – The surface roughness varies during Ag^+ cementation on solid Cu. At the beginning of the process, a decrease in surface roughness is observed in both O_2-free and O_2-saturated solutions. The flattening effect of Ag cement deposited on the Cu surface is responsible for this decrease. Further on, an increase in surface roughness appears. Under aerobic conditions, the effective surface area of cathodic sites is mainly responsible for the increase of the surface roughness. This effect is especially pronounced in solutions with a high initial Ag^+ concentration (100 mg/dm^3). Under anaerobic conditions, the surface roughness does not change significantly from a certain moment on, and the observed rate enhancement is induced mainly by a competitive chemical process between Ag^+ and Cu^+ ions.

Our study clearly shows that distribution diagrams of surface heights can provide useful information on the surface roughness at various stages of Ag-deposit formation, and, consequently, can be related to the kinetics of cementation. Qualitative data on surface roughness obtained for O_2-free and O_2-saturated solutions can be linked with the influence of the presence of O_2 on the mechanism of the process. Especially, surface-height-distribution diagrams provide unique information in systems with a very low concentration of the noble metal, where formation of dendrites does not occur. The method can be employed successfully to study the evolution of surface roughness during cementation.

REFERENCES

[1] S. H. Castro, M. Sánchez, *J. Cleaner Prod.* **2003**, *11*, 207.
[2] F. A. López, M. I. Martín, C. Pérez, A. López-Delgado, F. J. Alguacil, *Water Res.* **2003**, *37*, 3883.
[3] M.-S. Lee, J.-G. Ahn, J.-W. Ahn, *Hydrometallurgy* **2003**, *70*, 23.
[4] A. Dib, L. Makhloufi, *Chem. Eng. Process.* **2004**, *43*, 1265.
[5] A. A. Mubarak, A. H. El-Shazly, A. H. Konsowa, *Desalination* **2004**, *167*, 127.
[6] J. R. Parga, R. Y. Wan, J. D. Miller, *Miner. Metall. Process.* **1988**, *5*, 170.
[7] C. A. Fleming, *Hydrometallurgy* **1992**, *30*, 127.
[8] H. Y. Lee, S. Y. Kim, J. K. Oh, *Can. Metall. Quart.* **1997**, *36*, 149.
[9] J. Ornelas, M. Marquez, J. Genesca, *Hydrometallurgy* **1998**, *47*, 217.
[10] G. V. Gamboa, M. M. Noyola, A. L. Valdivieso, *Hydrometallurgy* **2005**, *76*, 193.
[11] G. V. Gamboa, M. M. Noyola, A. L. Valdivieso, *J. Colloid Interface Sci.* **2005**, *282*, 408.
[12] T. M. Dreher, A. Nelson, G. P. Demopoulos, D. Filippou, *Hydrometallurgy* **2001**, *60*, 105.
[13] B. B. Boyanov, V. V. Konareva, N. K. Kolev, *Hydrometallurgy* **2004**, *73*, 163.
[14] J. Näsi, *Hydrometallurgy* **2004**, *73*, 123.
[15] Y. Ku, M.-H. Wu, Y.-S. Shen, *Waste Manage.* **2002**, *22*, 721.
[16] S. A. Nosier, *Chem. Biochem. Eng. Q.* **2003**, *17*, 219.
[17] M. El-Batouti, *Anti-Corrosion Methods Mater.* **2005**, *52*, 42.
[18] N. T. Pham, M. Aurousseau, F. Gros, P. Ozil, *J. Appl. Electrochem.* **2005**, *35*, 249.
[19] E. A. von Hahn, T. R. Ingraham, *Trans. Metall. Soc. AIME* **1967**, *239*, 1895.
[20] P. H. Strickland, F. Lawson, *Proc. Austr. Inst. Miner. Metall.* **1971**, *237*, 71.

[21] J. Ke, L. Yue, *Acta Metall. Sin.* **1984**, *20*, A197.
[22] B. Waligóra, Z. Görlich, J. Hotloś, M. Jaskuła, Badanie początkowych etapów cementacji jonów srebra miedzią metaliczną – Report of Investigation No. CPBP 03.08, zadanie I.2.9, Kraków, 1990 (in Polish).
[23] L. Makhloufi, S. Bourouina, S. Haddad, *Electrochim. Acta* **1992**, *37*, 1779.
[24] N. Ramesh, B. S. Sheshadri, *Indian J. Technol.* **1992**, *30*, 19.
[25] N. Ramesh, B. S. Sheshadri, *Trans. Met. Finish. Assoc. India* **1992**, *1*, 53.
[26] G. Puvvada, T. Tran, *Hydrometallurgy* **1995**, *37*, 193.
[27] I. M. Ritchie, S. G. Robertson, *J. Appl. Electrochem.* **1997**, *27*, 59.
[28] C. Alemany, M. Aurousseau, F. Lapicque, P. Ozil, *J. Appl. Electrochem.* **2002**, *32*, 1269.
[29] I. M. Ritchie, W. P. Staunton, Proceedings of the 1st International Symposium on Electrochemistry in Mineral and Metal Processing, Pennington, New York, 1984, p. 486–500.
[30] G. D. Sulka, M. Jaskuła, *Hydrometallurgy* **2003**, *70*, 185.
[31] G. D. Sulka, M. Jaskuła, *Hydrometallurgy* **2005**, *77*, 131.
[32] G. D. Sulka, M. Jaskuła, *Hydrometallurgy* **2002**, *64*, 13.
[33] G. D. Sulka, M. Jaskuła, *Hydrometallurgy* **2004**, *72*, 93.
[34] http://www.nanotec.es.

Received January 13, 2006